Contents list available at CBIORE journal website

International Journal of Renewable Energy Development

Journal homepage: https://ijred.cbiore.id

Research Article

Application of day-ahead optimal scheduling model based on multi-energy micro-grids with uncertainty in wind and solar energy and energy storage station

Hongxin Zhang *

School of Electrical Engineering, Nanjing Vocational University of Industry Technology, Nanjing, 210023, China

Abstract. Multi-energy micro-grid has received widespread attention in the wave of continuous promotion and development of renewable energy. However, in the face of wind and solar uncertainty, its scheduling model needs to be further optimized. Therefore, a multi-energy micro-grid day-ahead optimal scheduling model was proposed to construct wind and solar uncertainty scenarios, and the application of energy storage station was considered. Multiple algorithms were introduced to propose the multi-energy micro-grid day-ahead optimal scheduling model. Finally, the research content was validated. The results confirmed that the wind and solar power output probability model could describe the characteristics of wind and solar power output at different periods. The generated scenes had a large number of wind speeds in the range of 1.5 m/s to 5 m/s, and the light intensity reached its peak at 14:00, which was consistent with the historical data of the research object. In addition, the total pre-scheduling cost of this optimized scheduling model within a day was 45.16×10^5 yuan, while the actual scheduling cost within a day was only 21.46×10^5 yuan. It saved costs by 41.65% and 44.95%, respectively, compared to the comparison algorithms. The research has driven innovation and optimization of the multi-energy micro-grid scheduling model. This provides a useful theoretical and practical basis for addressing the uncertainty of wind and solar energy and improving the economic efficiency of energy systems, which is crucial for the sustainable development of new energy.

Keywords: Wind and solar uncertainty; Multi-energy micro-grid; Energy storage station; Optimal scheduling; Probability model

Received: 29th March 2024; Revised: 16th June 2024; Accepted: 6th July 2024; Available online: 15th July 2024

1. Introduction

Under the rapid development of modern society, traditional disposable energy is constantly decreasing. The sustainable development and energy security of energy systems have become one of the major challenges that today's society faces (Maka and Alabid, 2022). In addition, the intensification of global warming, environmental pollution and other issues has led people to urgently seek more environmentally friendly, clean, and sustainable energy (Kostis *et al.*, 2023). Many countries, led by China, have elevated "carbon neutrality" to a national strategy and proposed the era goals of "peaking carbon" and "carbon neutrality" (Vasilj *et al.*, 2020). In this context, Multi-Energy Micro-Grid (MEMG) has emerged. In addition, Renewable Energy (RE) such as wind and solar energy are increasingly being used in production and daily life, which has to some extent alleviated the pressure of primary energy use (Yodo and Arfin, 2021). However, due to the strong seasonal and weather fluctuations of wind and solar energy, MEMG faces many challenges. It is crucial to predict and adapt to the uncertainty of wind and solar energy in advance to achieve efficient operation of MEMG. Energy Storage Station (ESS) is a key component of MEMG, which converts electrical energy into other forms of energy and converts it back into electrical energy when needed (Kamath *et al.*, 2020). ESS can compensate for the volatility and intermittency of RE by storing energy, improving the stability and reliability of micro-grids (Moradzadeh and Abdelaziz, 2020). Therefore, the study aims at economic costs and Carbon Emission (CE) and proposes a Wind and Solar Power Output Probability Model (WSPOPM) for Wind and Solar Uncertainty (WSU). On this basis, considering the role of ESS in MEMG, a Multi-Energy Micro-Grid Day-Ahead Optimal Scheduling (MEMG-DAOS) model is proposed. The research aims to improve the operational efficiency of MEMG systems by optimizing scheduling models to adapt to the future trend of carbon neutral energy development.

The study is divided into four parts. Firstly, the current research on RE, MEMG, and other related topics is introduced. Secondly, it mainly introduces how to build WSPOPM and MEMG-DAOS. Then, experimental verification is conducted on the performance of the proposed WSPOPM and MEMG-DAOS, demonstrating their effectiveness and feasibility. Finally, the article is summarized and discussed, and the shortcomings and future prospects of this paper are pointed out.

2. Related works

As time goes by, the proportion of RE in energy supply is gradually increasing, including but not limited to the utilization of RE such as solar energy, wind energy, hydropower,

*Corresponding author
Email: 2011100730@niit.edu.cn (H. Zhang)

https://doi.org/10.61435/ijred.2024.60218
ISSN: 2252-4940/© 2024.The Author(s). Published by CBIORE

geothermal energy, etc. However, the use of RE often comes with various uncertainties. Therefore, many scholars have conducted research on such issues. The fluctuation of RE and load output power can bring problems to the scheduling and operation of the distribution network. Zhao *et al.* proposed a robust voltage control model based on an improved generative adversarial network. Meanwhile, they introduced an improved wolf pack algorithm to improve the model accuracy. This effectively improved the convergence speed, accuracy, and stability of robust voltage control (Zhao *et al.*, 2020). Faraji *et al.* proposed an optimized scheduling and operation method for permanent magnet generators to address the uncertainty of equipment such as wind turbines. They generated different scenarios through Monte Carlo simulation, thereby significantly improving the robustness of micro-grids in the face of uncertainty (Faraji *et al.*, 2020). The integrated energy system in distributed generators has output uncertainty and is limited by CE. Ge *et al.* proposed a novel optimization planning model that considered both the uncertainty of distributed power generation output and CE penalties. This effectively reduced the impact of uncertainty and CE (Ge *et al.*, 2021). Yang *et al.* proposed a time-series joint scheduling method to address the uncertain risks faced by grid energy storage demand resources in active distribution networks. They made full use of various resources in terms of spatial and temporal data, completed analysis of the future, and effectively reduced the risk of energy storage in the power grid (Yang *et al.*, 2020).

MEMG is a small-scale energy system designed to provide electricity, thermal energy, and other forms of energy services by integrating multiple energy resources and equipment. Compared with traditional single-energy micro-grids, MEMG has higher integration and diversity. It has emerged under the pursuit of sustainability, cleanliness, and reliability of energy systems, as well as the promotion of technological progress. Similarly, many scholars have conducted extensive research on it. MEMG has the problem of multi-stage real-time random operation. Therefore, Li *et al.* proposed a solution that combined hybrid model predictive control and approximate dynamic programming methods. A good real-time operation solution was obtained, improving the control of MEMG by continuously updating predictions (Li *et al.*, 2021). Tian *et al.* proposed an optimized scheduling model based on unified energy flow to address the low planning efficiency of coordinated operation in MEMG. They established a simulated energy storage model to describe the time-dependent characteristics of MEMG. This provided an effective new method for scheduling optimization of MEMG (Tian *et al.*, 2020). Masrur *et al.* proposed a mixed integer linear optimization model to address the challenge of integrating multiple energy sources in MEMG. They calculated and predicted the hourly electricity and thermal load curves. This achieved coordinated operation of multiple energy sources and improved the recovery ability of MEMG in the event of long-term power outages in the power grid (Masrur *et al.*, 2022). There are various uncertainties in RE power generation, electricity prices, and load demand. Therefore, Chen *et al.* proposed a two-stage stochastic operation scheme for optimizing the scheduling of distributed generators, electric boilers, electric refrigerators, and energy storage equipment. Meanwhile, they borrowed a mixed integer linear programming model to save operating costs while maintaining the robustness of MEMG and the thermal comfort of customers (Chen *et al.*, 2020).

In summary, many scholars around the world have considered the uncertainty of RE utilization and conducted multiple research works to solve these problems. In addition, as an emerging energy system, the importance of MEMG is self-evident. However, in the face of WSU, the optimization scheduling of MEMG is rarely discussed. Poor scheduling solutions can lead to waste of micro-grid operating costs, resources, etc., hindering the achievement of "carbon peak" and "carbon neutrality" goals. Therefore, based on WSPOPM, the study proposes MEMG-DAOS with economic costs and CE as optimization objectives, providing a comprehensive and innovative solution to address the uncertainty and operational efficiency issues in actual MEMG systems.

3. Day-ahead optimal scheduling model with multi-energy micro-grid and energy storage station based on wind and solar uncertainty

Driven by the goals of global energy transformation and carbon neutrality, this section introduces in detail an innovative day-ahead optimization scheduling model, MEMG-DAOS, proposed in this study. Aiming at the operational challenges of MEMG under the influence of wind and solar energy uncertainties, this model improves the scheduling efficiency and economy of the system by establishing WSPOPM and introducing advanced optimization algorithms. At the same time, it enhances the adaptability to RE fluctuations and the low-carbon operation characteristics of the micro-grid.

3.1 Wind and solar power output probability model and scene generation

A MEMG-DAOS model considering economic costs and CE is proposed for WSU. It needs to consider the time scale of wind speed and light intensity. Therefore, WSPOPM is established in this study to provide typical scenario inputs for the model and achieve optimized scheduling of MEMG. In WSPOPM, wind power generation system and photovoltaic power generation system are modelled. weibull distribution is used to describe the power output characteristics of wind turbines, while Bate distribution is used to simulate the output of photovoltaic power generation system. The maximum likelihood method is used to estimate the parameters of these distribution models to ensure that the models can accurately reflect the probabilistic characteristics of wind speed and light intensity. The Latin Hypercube sampling method combined with K-means clustering method is used to select representative scenes from a large number of generated scene-power scenes to reduce the computational burden of subsequent optimization models and maintain the diversity of scenes. Firstly, the wind power generation system and photovoltaic power generation system are modelled. Figure 1 shows the typical structure of wind turbines and photovoltaic power generation systems (Chen *et al.*, 2021; Nosratabadi *et al.*, 2021).

In Figure 1 (a), the wind turbine includes pneumatic, transmission, electrical, and control systems. During the operation of wind turbine, its power acquisition is limited by both the limits of the pneumatic and electrical systems (Liu *et al.*, 2020; Zhang *et al.*, 2021). Its normal output power characteristic P_w, which is the relationship between wind speed and fan output, is represented by equation (1).

$$P_w = \begin{cases} 0(v < v_{ci}) \\ P_r \frac{v^3 - v_{ci}^3}{v_r^3 - v_{ci}^3}(v_{ci} < v < v_r) \\ P_r(v_r < v < v_{co}) \end{cases} \quad (1)$$

In equation (1), P_r is the rated power. v, v_{ci}, v_r, and v_{co} represent the actual wind speed, cut in wind speed, rated wind speed, and cut out wind speed, respectively (Li *et al.*, 2021; Li *et*

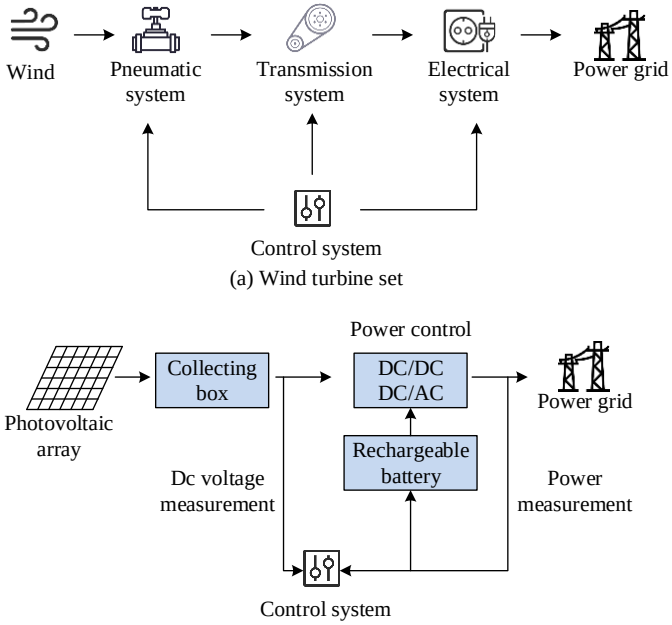

(a) Wind turbine set

(b) Photovoltaic power generation system

Fig 1 Typical structure of wind power generation system and photovoltaic power generation system

al., 2020). The study uses probability models to fit wind turbine output, with the aim of reflecting more wind power prediction information. The research suggests that the wind power generation system model conforms to a Weibull distribution, and the probability density function $\Phi_w(v)$ of wind speed and the corresponding probability distribution function $\varphi_w(v)$ are represented by equation (2).

$$\begin{cases} \Phi_w(v)=\left(\frac{k}{c}\right)\left(\frac{v}{c}\right)^{k-1}\exp\left[-\left(\frac{v}{c}\right)^k\right] \\ \varphi_w(v)=1-\exp\left[-\left(\frac{v}{c}\right)^k\right] \quad (k>0,c>1) \end{cases} \tag{2}$$

In equation (2), k represents the shape parameter. c is a scale parameter. The maximum likelihood method is used to solve the equation and obtain the values of k and c. The likelihood function is represented by equation (3).

$$L(k,c)=\prod_{i=1}^{n}\left(\frac{k}{c}\right)\left(\frac{v}{c}\right)^{k-1}\exp\left[-\left(\frac{v}{c}\right)^k\right] \tag{3}$$

In equation (3), the values of k and c are solved using equation (4).

$$\begin{cases} F_1=\frac{\partial L(k,c)}{\partial(k)}=0 \\ F_2=\frac{\partial L(k,c)}{\partial(c)}=0 \end{cases} \rightarrow \begin{cases} F_1=\sum_{i=1}^{n}\left[\frac{1}{k}+\ln v_i-\ln c-\left(\frac{v_i}{c}\right)^k\ln\frac{v_i}{c}\right]=0 \\ F_2=\sum_{i=1}^{n}\left[-\frac{k}{c}+\frac{k}{c}\left(\frac{v_i}{c}\right)^k\right]=0 \end{cases} \tag{4}$$

In equation (4), v_i represents the statistical data of wind speed samples. To use the maximum likelihood method, it is first necessary to collect v_i and obtain the initial values of the shape and distribution parameters. Then, the Jacobian matrices of F_1 and F_2 are calculated, and the changes of k and c are obtained. The current parameter estimate has been updated using changes and gradually approximated to the true maximum likelihood estimate. If the change meets the accuracy requirements, the calculation of k and c values is completed. Thus, the modeling of the wind power generation system in WSPOPM is successful. In Figure 1 (b), the composition of the photovoltaic power generation system includes a photovoltaic array, DC/DC converter, DC/AC inverter, battery, and control system. A photovoltaic array is composed of multiple photovoltaic cells. The electrical energy is transmitted to the DC/DC and DC/AC links through a combiner box and ultimately converted into AC energy that meets the requirements of the power grid (Hou *et al.*, 2021; Shaheen *et al.*, 2021; Su and Teh, 2022). The factors that affect the output of photovoltaic power generation include light intensity, weather temperature, air humidity, and atmospheric pressure. The power equation for photovoltaic power generation output is represented by equation (5).

$$P_{pv}=\eta_{pv}S_{pv}\theta_t \tag{5}$$

In equation (5), P_{pv} is the output of the photovoltaic system. η_{pv} and S_{pv} are the photovoltaic radiation efficiency and radiation area, respectively. θ_t means the solar radiation intensity at a certain moment. The research suggests that the photovoltaic power generation system model follows a bate distribution, and its shape parameter α and distribution parameter β are represented by equation (6).

$$\begin{cases} \alpha=\frac{\mu\beta}{1-\mu} \\ \beta=(1-\mu)\left(\frac{\mu(1-\mu)}{\sigma^2}-1\right) \end{cases} \tag{6}$$

In equation (6), μ and σ represent the expected value and standard deviation of photovoltaic radiation intensity, respectively. Thus, the establishment of the photovoltaic power generation system model in WSPOPM is completed. Furthermore, the study utilizes an improved Monte Carlo statistical simulation method, Latin Hypercube Sampling (LHS), to establish wind and solar power output uncertainty scenarios,

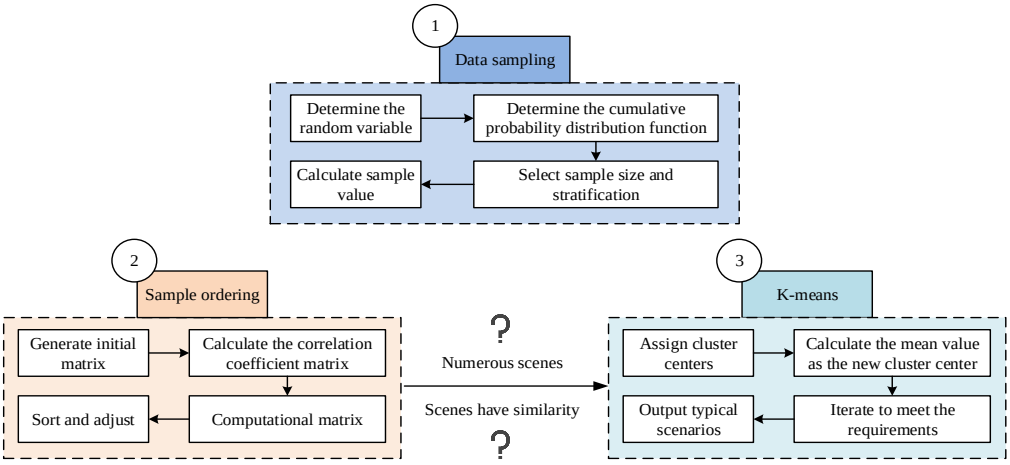

Fig 2 Generation method of wind-power uncertainty scene

and utilizes K-means clustering method to reduce the scenes. The main reason for choosing the K-means algorithm is that it can effectively identify and summarize the representative typical scenes from a large number of scenery and power scenes, while maintaining the high efficiency and practicality of the processing process (Liu *et al.*, 2020; Nowak *et al.*, 2020). By iteratively optimizing the cluster center, the K-means algorithm ensures the homogeneity within each cluster and the obvious differences between clusters, which not only helps to capture the diversity of the wind power uncertainty, but also significantly reduces the computational complexity and solution time of the subsequent optimization model by reducing the number of scenes (Shirzadi *et al.*, 2022; Xu *et al.*, 2021). In addition, as a mature and widely used clustering method, K-means has the advantage of being easy to implement and adjust parameters, which can improve the practicality of the model and the accuracy of optimal scheduling (Liu and Yang , 2021; Wu *et al.*, 2021). Figure 2 shows the specific process.

In Figure 2, establishing a scenario of wind and solar power output uncertainty mainly involves three steps. Firstly, for data sampling, it is necessary to determine the value of the random variable X_k and its cumulative probability distribution function F. Subsequently, LHS is used to divide the probability density function of wind speed into N equal intervals based on sample size. Finally, the values of the midpoints in each interval are calculated. The second step is sample sorting, which generates a matrix L. The value of each row represents the sample location information of X_k. After matrix factorization, the lower triangular matrix D is obtained. Then, the correlation coefficient matrix ρ and matrix G are calculated, represented by equation (7).

$$\begin{cases} \rho = L \cdot D \cdot D^T \\ G = D^{-1} \cdot L \end{cases} \tag{7}$$

The elements in L are arranged according to the size of the elements in G, and the positions of each element in the sample matrix X are adjusted, resulting in a simulation scene composed of a large number of sampling points with weak correlation. However, there are many scenes generated by LHS, and many scenes have certain similarities. Therefore, in the third step, the study uses K-means to first determine the number of sets in the initial state and assign initial cluster centers. Then, the samples in the typical scene set are calculated and assigned to the nearest cluster center (Haidar *et al.*, 2020; Tian *et al.*, 2020). Subsequently, the average value of scene coordinates under each cluster is calculated as the new center. Iterations are carried out repeatedly until the cluster center no longer moved widely or met the requirements for iterations. Ultimately, the study aims to output wind and solar scenes with typical features as inputs to MEMG-DAOS, improving the accuracy of the model.

3.2 Establishment of a multi-energy micro-grid day-ahead optimal scheduling model

Faced with WSU, MEMG may face challenges such as unstable power output, increased complexity of operation scheduling, rising energy storage demand, cost management challenges, and power supply reliability issues (Das *et al.*, 2020; Liu *et al.*, 2020). This uncertainty makes it more difficult for the system to adapt to different wind and solar conditions, thus forming a vicious cycle. Therefore, on the basis of the WSPOPM model, MEMG-DAOS is further established. The model considers the flow of electric energy and heat energy in MEMG, especially the role of ESS in the system, as well as the energy conversion and storage state during its charge-discharge process. The model aims to minimize the total cost and CE, covers the cost of electricity purchase, natural gas purchase, equipment operation and maintenance, and sets the corresponding constraints to ensure the safety and reliability of the system. In order to improve the speed and accuracy of optimal scheduling, the non-dominated sorting genetic algorithm II (NSGA-II) is introduced into the model to deal with multi-objective optimization problems and find the balance point between economic and low-carbon objectives. The establishment of MEMG-DAOS model provides an effective day-ahead optimization scheduling strategy for MEMG in the face of wind-wind uncertainty, which helps to improve the operating efficiency and economy of the system. The study first demonstrates the basic structure of MEMG in Figure 3.

In Figure 3, the basic structure of the MEMG established in this study includes electrical energy flow and thermal energy flow, where electrical energy involves ESS. In ESS, energy storage components can store or release electrical energy through the conversion between chemical and electrical energy and change their own energy storage state through charging and discharging. The study simplifies ESS and does not focus on the internal charging and discharging processes of electric energy storage components. The energy change of the electric energy storage element is represented by equation (8).

$$W_{ES}^{1} = W_{ES}^{0}\left(1-\sigma_{ES}\right) + \left(P_{ES\cdot C}\eta_{ES\cdot C} - \frac{P_{ES\cdot C}}{\eta_{ES\cdot C}}\right)\Delta t \tag{8}$$

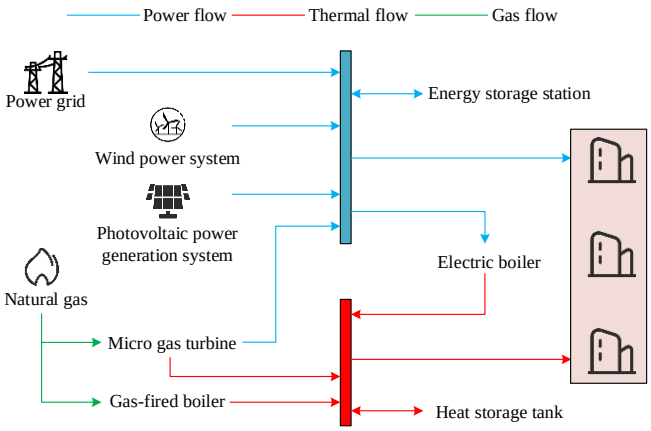

Fig 3 Basic structure of multi-energy micro-grid

In equation (8), W_{ES}^{0} and W_{ES}^{1} are the electricity levels before and after charging and discharging, respectively. σ_{ES} means self-discharge rate. $P_{ES\cdot C}$ and $\eta_{ES\cdot C}$ represent charging power and discharging power, respectively. $P_{ES\cdot D}$ and $\eta_{ES\cdot D}$ mean charging efficiency and discharging efficiency, respectively. Δt means charging and discharging time. Constraints are imposed on the electrical energy storage components in ESS in Figure 4.

In Figure 4, S is the state of charge of the energy storage element. $W_{ES\cdot R}$ means the rated capacity of the energy storage element. W_{ESmin} and W_{ESmax} represent the minimum and maximum energy storage of the electric energy storage element, respectively. $P_{ES\cdot Cmax}$ and $P_{ES\cdot Dmax}$ refer to the maximum charging power and maximum discharging power of the energy storage element, respectively. u_{ES} is a state variable, where 0 represents the discharge state and 1 represents the charging state. In the following research, MEMG-DAOS is established. The minimum daily operating cost of MEMG is calculated using equation (9).

$$C = min\left(C_{te} + C_{tf} + C_{tg}\right) \tag{9}$$

In equation (9), C represents the total cost. C_{te} is the cost of purchasing electricity. C_{tf} means the cost of purchasing natural gas. C_{tg} refers to the cost of equipment operation and maintenance. In addition to cost, the study also considers the constraint of minimizing CE, represented by equation (10).

$$F = \min\left(m_{MT\cdot gas} Q_{MT\cdot gas} + m_{GB} \frac{Q_{GB\cdot heat}}{\eta_{GB} CV_{gas}} + m_{gird} P_{gird\cdot t} \right) \Delta t \tag{10}$$

In equation (10), $m_{MT\cdot gas}$ represents the CE coefficient per unit of natural gas consumed. $Q_{MT\cdot gas}$ is the gas power. m_{GB} refers to the CE coefficient per unit of natural gas consumption. $Q_{GB\cdot heat}$ means the thermal power output. η_{GB} represents work efficiency. CV_{gas} is the unit calorific value of natural gas, with a value of 10 kWh/m^3. m_{gird} refers to the CE coefficient of power generation in the power grid system. $P_{gird\cdot t}$ means the amount of electricity purchased from the micro electric network during period t. Δt means within a certain period of time. In MEMG-DAOS, a data-driven approach is used to establish a functional relationship between output power and control variables from historical data of wind and solar energy. This allows MEMG to better understand how output power is influenced by control variables under different conditions. It further optimizes the output power more effectively, improves the performance and efficiency of the energy system, and extends to optimization methods for joint operation of multiple MEMGs based on MEMG operation optimization. MEMG-DAOS is represented by equation (11).

$$\begin{cases} \min\left(c^T x + \max\limits_{\substack{P\in D \\ x\in X}} E_p\left(e\left(x,\xi\right)\right)\right) \\ s.t. \begin{cases} e\left(x,\xi\right) = b^T y \\ y \in R \\ Ax + By + C\xi \le E \end{cases} \end{cases} \tag{11}$$

In equation (11), E_p represents the expected value. x is the set of decision variables in the first stage. y refers to

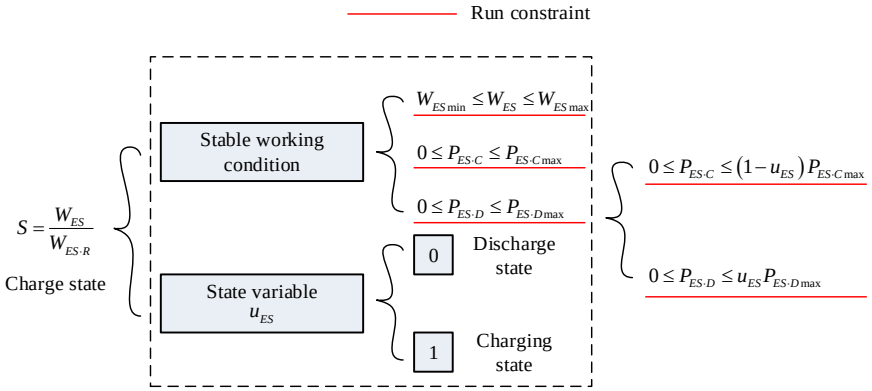

Fig 4 Constraint diagram of electric energy storage components

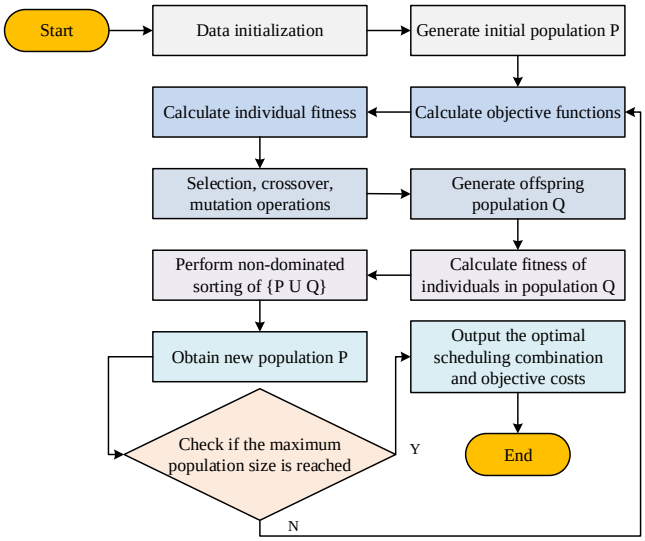

Fig 5 Flowchart of NSGA-II in MEMG-DAOS model

uncertain variables. ξ is the second stage variable. C, b, A, B, C, and E are the coefficient vectors or matrices corresponding to the variables in the optimization model, T represents the transpose symbol, D represents the data-driven set of uncertainties, and R is the constant. The cost function of MEMG during the pre-scheduling phase is represented by equation (12).

$$G_1 = C^G + C^{UD} + C^W + C^O + C^{EN} \tag{12}$$

In equation (12), C^G represents the cost of generating electricity for the unit. C^{UD} is the cost of starting and stopping the unit. C^W refers to the operation and maintenance cost of distributed power sources. C^O means equipment maintenance costs. C^{EN} represents environmental cost. Multiple micro-grid operators conduct real-time control based on the pre-scheduling plan and simultaneously consider the uncertainty of distributed power generation output and load power. The objective function is represented by equation (13).

$$G_2 = \Delta C^{G,UD} + \Delta C^{ESS} + \Delta C^{EX} + C^{LOSS} \tag{13}$$

In equation (13), $\Delta C^{G,UD}$ represents the cost of unit regulation. ΔC^{ESS} refers to the cost of ESS regulation. ΔC^{EX} is the transaction cost. C^{LOSS} means regulating the cost of wind curtailment. Finally, the study incorporates Non-Dominated Sorting Genetic Algorithm II (NSGA-II) into MEMG-DAOS to improve the speed and accuracy of optimization scheduling in Figure 5.

In Figure 5, NSGA-II first initializes the data and then selects the minimum operating cost and CE as the optimization objectives for operation. By processing constraint conditions and objective function operations through the corresponding running optimization vectors of individual populations, the calculation results of individual fitness can be obtained (Lee *et al.*, 2020; Shinde *et al.*, 2020). Based on the individual fitness results obtained in the previous steps, selection, crossover, and mutation operations are performed to obtain the individual situation of the next generation population. Subsequently, the fitness of all individuals in the current generation population is recalculated and a hierarchical operation is performed between the previous generation population and the contemporary population. When the set maximum number of genetic iterations is reached, the output result is the optimal scheduling power generation combination and various target costs.

4. Simulation and performance analysis of the multi-energy micro-grid day-ahead optimal scheduling model

4.1 Scheduling model setting and scenario simulation

To verify the effectiveness and superiority of MEMG-DAOS, a MEMG operation model was first constructed using the wind and solar output uncertainty scenario generated by WSPOPM. Subsequently, it underwent a day-ahead optimal

Table 1
Equipment parameters of an actual multi-energy micro-grid in northern China

Equipment	Technical parameter		Economic parameter	
Wind power system	Capacity	50kW	Operation and maintenance cost	0.0196 yuan/kWh
	Capacity	80kWp		
Photovoltaic system	Cut-in wind speed	2.5m/s	Operation and maintenance	0.0235 yuan/kWh
	Rated wind speed	12m/s		
	Cut-out wind speed	18m/s		
	Capacity	150kWh		
	Charging efficiency	0.95		
	Discharge efficiency	0.95		
	Self-discharge rate	0.04		
ESS	Minimum energy storage	5kWh	Operation and maintenance	0.0018yuan/kWh
	Maximum storage energy	140kWh		
	Maximum charging power	20kW		
	Maximum discharge power	20kW		
	Initial storage energy	100kWh		

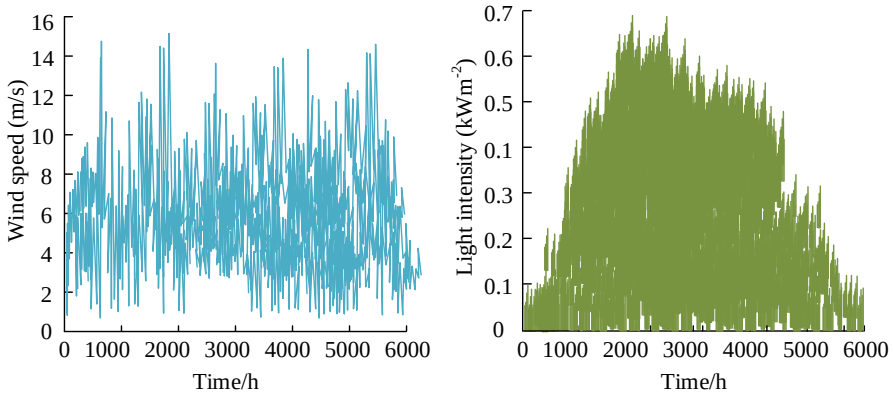

(a) Wind distribution (b) Light intensity distribution

Fig 6 Parameter fitting values in WSPOPM

scheduling. The study selected a practical grid connected MEMG in northern China as the research object. Table 1 shows the parameters of wind turbines, photovoltaics, and ESS equipment.

Table 1 details the key equipment parameters of an actual grid-connected MEMG in North China, including the capacity of wind power system and photovoltaic power system and their operation and maintenance costs. The capacity of wind power system is 50 kW, the operation and maintenance cost is 0.0196 yuan/kWh, and the capacity of photovoltaic system is 80 kWp at its peak. Operation and maintenance cost is 0.0235 yuan/kWh. The wind power system also includes specific technical parameters, such as the cut wind speed of 2.5 m/s, the rated wind speed of 12 m/s and the cut wind speed of 18 m/s. The parameters of the ESS range from 150 kWh storage capacity to 0.0018 yuan/kWh operation and maintenance costs, with both charge and discharge efficiency of 95%, self-discharge rate of 4%, minimum and maximum storage energy of 5 kWh and 140 kWh, respectively, and maximum charge and discharge power of 20 kWh. In addition, the energy storage system starts operation with an initial power of 100 kWh. These detailed technical and economic parameters are the basis for the optimization of MEMG scheduling, ensuring that the system can carry out effective day-ahead optimization scheduling under the uncertainty of wind and solar energy to improve operational efficiency and economy (Kalakova *et al.*, 2021; Naughton *et al.*, 2021). To better accommodate wind and solar RE, the MEMG is connected to the higher-level distribution network, allowing the purchase of electricity from the higher-level distribution network to meet the load demand in the MEMG. In addition, while allowing MEMG to sell surplus electricity to higher-level distribution networks and improve the economy of MEMG, it also demonstrates low-carbon characteristics. In Figure 6, the historical data of this MEMG are presented.

In Figure 6 (a), the wind speed distribution in the historical data is concentrated in the range of 0 m/s–14 m/s and concentrated in the 0 m/s–6 m/s. In Figure 6 (b), the highest light intensity is around 0.7 kWm^{-2}. The study utilized the distribution of wind speed and light intensity of the MEMG to fit the shape k of wind speed, scale c, shape α of light intensity, and distribution parameter β in Figure 7.

In Figure 7 (a), k shows an upward trend from 1 to 7 hours, a downward trend from 7 to 18 hours, and an upward trend again from 18 to 24 hours, with a significant change. c has a relatively small change range within 24 hours, and the overall trend of change is similar to k. In Figure 7 (b), both α and β suddenly and rapidly increase after 6h-7h, while suddenly and rapidly decrease between 16h-18h, which is consistent with the changes in light intensity within a day. Furthermore, the study utilized WSPOPM to generate 200 wind speed scenes and 200 lighting intensity scenes and used K-means to reduce a total of 400 scenes. Finally, 10 typical wind speed scenes and 10 typical lighting intensity scenes are retained in Figure 8.

In Figure 8 (a), the generated scene has a higher number of wind speeds in the range of 1.5m/s to 5m/s. The number of wind speed time periods at 8m/s is relatively small, and the 10 generated scenarios matches the real data distribution, which has credibility. In Figure 8 (b), the distribution characteristics of the 10 lighting intensity scenes are also consistent with the true lighting intensity scenes. The light intensity starts to rise around

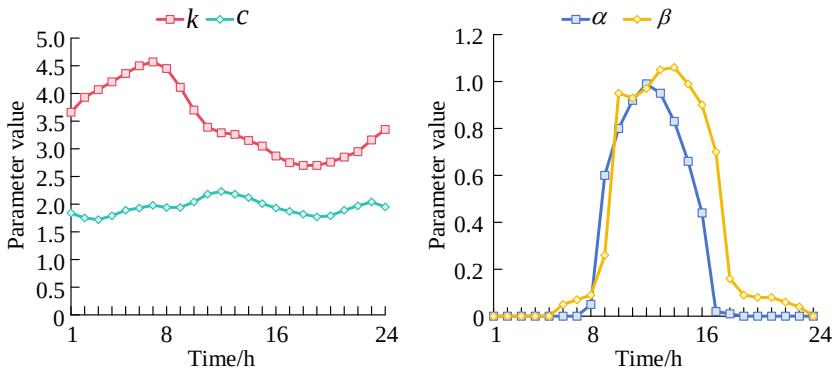

(a) Wind power system (b) Photovoltaic power generation system

Fig 7 Parameter fitting values in WSPOPM

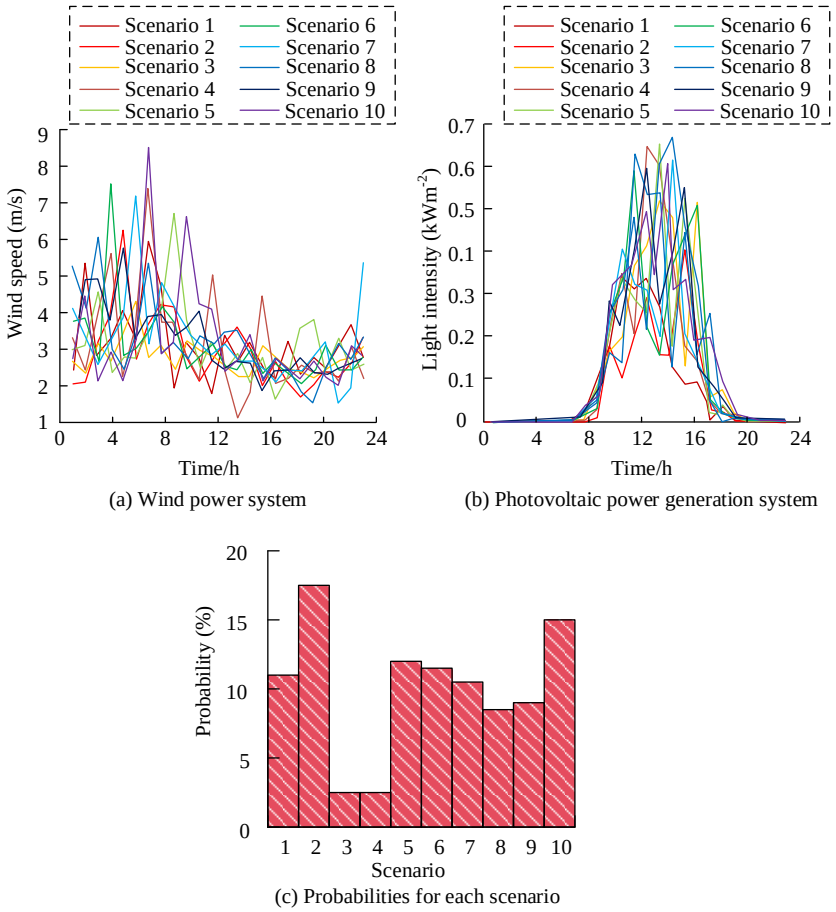

(a) Wind power system (b) Photovoltaic power generation system

(c) Probabilities for each scenario

Fig 8 10 typical wind speed scenes and 10 typical light intensity scenes

8:00 and reaches the peak of the day's light intensity around 14:00, until the light intensity approaches 0 around 18:00. In Figure 8 (c), among the 10 scenic scenes, scenario 2 has the highest probability of occurrence, reaching 17.50%, while scenarios 3 and 4 have the lowest probability of occurrence, only 2.5%.

4.2 Scheduling model performance analysis and verification

According to the above content, the study used scenario 2 as a simulated WSU scene for MEMG scheduling. The simulation experiment software used in the study is MATLAB 2016a. The hardware environment is mainly as follows. The CPU is Intel Core I5-7500, with a 6-core processor and 8GB of memory. Scenario 2 was input into MEMG-DAOS, economic goals and low-carbon goals were considered, and the day-ahead scheduling of MEMG was optimized using NSGA-II in the model. The study set the NSGA-II2 population to 200, with 100 iterations. Figure 9 shows its economic and low-carbon optimization results.

The optimization results shown in Figure 9 deeply reveal the complex trade off between CE and economic costs in day-ahead optimal scheduling of MEMG. Specifically, when the economic cost is in the range of 1700 yuan to 1750 yuan, CE is maintained at 1900kg to 1950kg, reflecting that within this cost range, each increase in a certain amount of economic input can achieve a relatively limited CE reduction effect. However, when the economic cost is close to 1950 yuan, CE shows a significant decline, falling below 1700kg, indicating that the additional

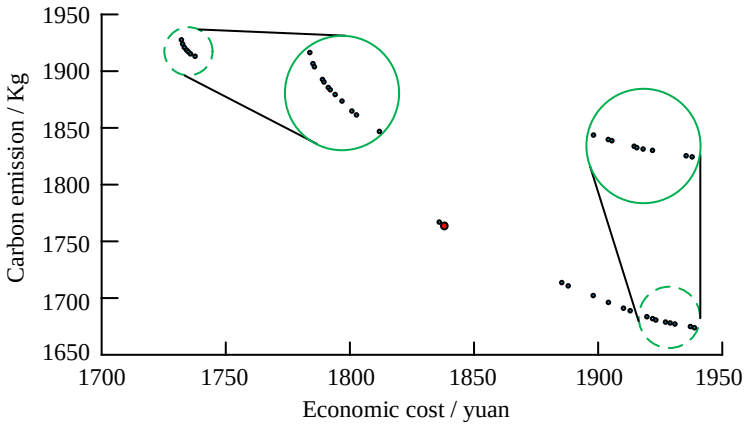

Fig 9 Optimization results of multi-energy micro-grid operation scheduling

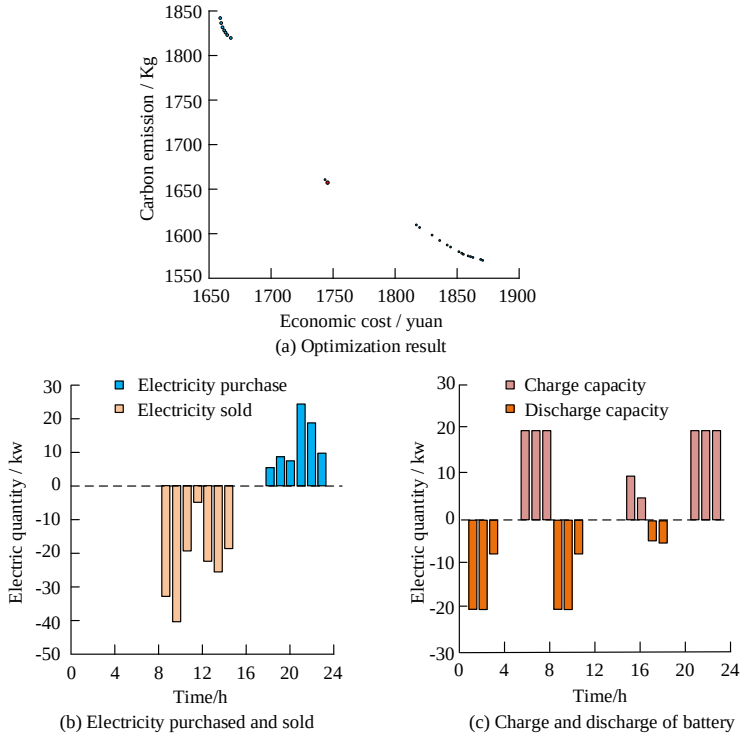

(a) Optimization result

(b) Electricity purchased and sold

(c) Charge and discharge of battery

Fig 10 Optimization results and electricity variation

economic input can bring about a significant reduction in CE when approaching the cost sensitive point (Yapici, 2021). Therefore, after comprehensive consideration, the study chose the location of the red dot in Figure 9. This point is more advantageous for MEMG operators in terms of economic cost compared to operating points with low CE. Compared to low-cost operating points, the CE of this selected operating point was more advantageous in the context of dual carbon. It could lay the groundwork for the carbon trading market and enhance the economic benefits brought by subsequent CE exchanges. On this basis, adjustments were made to the ESS by setting the battery capacity in the ESS to 100 kWh. Figure 10 shows the optimization results and changes in battery capacity.

The analysis results in Figure 10 show the interaction between economic cost and CE of MEMG after ESS adjustment and the effect of optimal scheduling strategy. First of all, Figure 10(a) reveals that after ESS adjustment, although the economic cost increases by 26.48 yuan compared with the previous one, the increase in cost results in a significant reduction of CE by 19.68kg, which indicates that by reasonably adjusting the energy storage strategy, the system operation efficiency can be ensured while the environmental impact can be effectively reduced. Figure 10(b) shows the electrical energy trading behaviour of MEMG at different time periods of the day. From 9:00 to 15:00, MEMG uses its own power generation capacity to sell electricity to the distribution network, which not only brings economic benefits, but also shows negative CE characteristics due to its use of RE. From 19:00 to 24:00, due to the increase in load demand, MEMG begins to purchase electricity from the distribution network to meet its own needs. Figure 10(c) details the operating state of the battery at different electricity price periods. During the valley periods when electricity prices are lower, such as 06:00 to 08:00, 16:00 to 17:00 and 21:00 to 24:00, the battery is charged and stores energy for use during peak

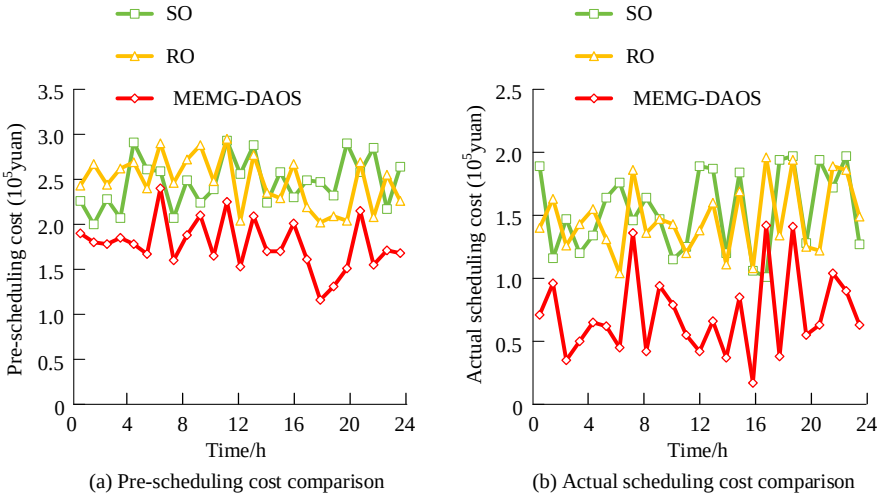

(a) Pre-scheduling cost comparison

(b) Actual scheduling cost comparison

Fig 11 Cost comparison result

hours. On the contrary, during the peak period of high electricity prices, such as 09:00 to 11:00, the battery is discharged, and the stored energy is fed back to the grid to achieve electricity sale, thereby improving the economy of the system. This strategy leads to an increase in economic costs, as the reduction in storage capacity limits the amount of power purchased during the price trough and increases the amount purchased during the peak period (Nagarajan *et al.*, 2020; Kanellos, 2020). At the same time, overall CE has been reduced by reducing the amount of electricity purchased from distribution. Finally, the study introduced Stochastic Optimization (SO) and Robust Optimization (RO) as comparative algorithms for MEMG-DAOS and compared the pre-scheduling cost and real-time control cost of MEMG in Figure 11.

The results of the analysis in Figure 11 highlight the significant benefits of MEMG-DAOS in terms of cost control. From Figure 11 (a), in the calculation of pre-scheduling cost, the MEMG-DAOS model shows its cost-effectiveness, which is always lower than the cost of SO method and RO method for scheduling. Specifically, at 0, the pre-scheduling cost of the MEMG-DAOS model is 1.94×10^5 yuan, compared to 2.26×10^5 yuan for the SO method and 2.81×10^5 yuan for the RO method, which indicates that at a single time point, the MEMG-DAOS model has achieved cost savings. Extending the perspective to the whole day, the total pre-scheduling cost of the MEMG-DAOS model is 45.16×10^5 yuan, which remains low in the all-day scheduling. Furthermore, from Figure 11 (b), for the actual dispatch cost, the total cost of MEMG-DAOS model in a day is only 21.46×10^5 yuan, which saves 41.65% and 44.95% of the cost compared with 36.78×10^5 yuan of SO method and 38.98×10^5 yuan of RO method, respectively. In summary, the conclusions of Figure 11 highlight the cost-effectiveness and efficiency of the MEMG-DAOS model for day-ahead optimal scheduling of MEMG, proving that the model is an effective tool to provide economically viable and environmentally sustainable scheduling solutions for MEMG operators under uncertain conditions.

5. Conclusion

In response to the WSU faced in MEMG, a WSPOPM was established in this paper to lay the groundwork for generating WSU simulation scenarios. After generating a large number of scenes, K-means was utilized in this study to reduce the scenes and obtain typical scenes, further proposing MEMG-DAOS. MEMG was mathematically modelled and NSGA-II was introduced to improve the speed and accuracy of optimized scheduling. Finally, an experiment was conducted. The experimental results of an actual grid connected MEMG in northern China confirmed that the overall trend of parameters k and c was similar. They showed an upward trend from 1h to 7h, a downward trend from 7h to 18h, and an upward trend from 18h to 24h, but the change amplitude of c was smaller. α and β almost suddenly increased rapidly after 6-7 h, and suddenly decreased rapidly between 16h-18h. WSPOPM could effectively calculate the historical data of MEMG. The wind speed and light intensity in the generated scene matched the historical data trend. In addition, the adjustment of ESS by MEMG-DAOS could effectively affect the economic cost and low-carbon goals of MEMG. Finally, the cost of MEMG-DAOS was always lower than that of SO and RO methods. For actual scheduling costs, MEMG-DAOS only cost 21.46×10^5 yuan per day, while SO and RO methods are 36.78×10^5 yuan and 38.98×10^5 yuan, respectively. Overall, this study can analyse WSU and complete the day-ahead optimization scheduling of MEMG, effectively reducing the operating cost of MEMG. However, further research can consider the impact of demand side load uncertainty and electricity price uncertainty on MEMG optimization scheduling.

Funding

The research is supported by: Jiangsu Wind Power Engineering Technology Center Open Fund Project: Development of an integrated practical training platform for micro grids of wind and solar energy storage (Fund number: ZK22-03-11).

References

Chen, T., Bu, S., Liu, X., Kang, J., Yu, F. R., & Han, Z. (2021). Peer-to-peer energy trading and energy conversion in interconnected multi-energy microgrids using multi-agent deep reinforcement learning. *IEEE Transactions on Smart Grid, 13*(1), 715-727. https://doi.org/10.1109/TSG.2021.3124465.

Chen, Y., Feng, X., Li, Z., Xu, Y., & Miragha, A. (2020). Multi-stage coordinated operation of a multi-energy microgrid with residential demand response under diverse uncertainties. *Energy Conversion and Economics, 1*(1), 20-33. https://doi.org/10.1049/enc2.12002.

Das, T., Roy, R., & Mandal, K. K. (2020). Impact of the penetration of distributed generation on optimal reactive power dispatch. *Protection and Control of Modern Power Systems, 5*(4), 1-26. https://doi.org/10.1186/s41601-020-00177-5.

Faraji, J., Hashemi-Dezaki, H., & Ketabi, A. (2020). Optimal probabilistic scenario-based operation and scheduling of prosumer microgrids considering uncertainties of renewable energy sources. *Energy Science and Engineering, 8*(11), 3942-3960. https://doi.org/10.1002/ese3.788.

Ge, L., Liu, H., Yan, J., Zhu, X., Zhang, S., & Li, Y. (2021). Optimal integrated energy system planning with DG uncertainty affine model and carbon emissions charges. *IEEE Transactions on Sustainable Energy, 13*(2), 905-918. https://doi.org/10.1109/TSTE.2021.3139109.

Haidar, A. M. A., Fakhar, A., & Muttaqi, K. M. (2020). An effective power dispatch strategy for clustered microgrids while implementing optimal energy management and power sharing control using power line communication. *IEEE Transactions on Industry Applications, 56*(4), 4258-4271. https://doi.org/10.1109/TIA.2020.2992974.

Hou, H., Chen, Y., Liu, P., Xie, C., Huang, L., Zhang, R., & Zhang, Q. (2021). Multisource energy storage system optimal dispatch among electricity hydrogen and heat networks from the energy storage operator prospect. *IEEE Transactions on Industry Applications, 58*(2), 2825-2835. https://doi.org/10.1109/TIA.2021.3128499.

Kalakova, A., Nunna, H. K., Jamwal, P. K., & Doolla, S. (2021). A novel genetic algorithm based dynamic economic dispatch with short-term load forecasting. *IEEE Transactions on Industry Applications, 57*(3), 2972-2982. https://doi.org/10.1109/TIA.2021.3065895.

Kamath, D., Arsenault, R., Kim, H. C., & Anctil, A. (2020). Economic and environmental feasibility of second-life lithium-ion batteries as fast-charging energy storage. *Environmental Science and Technology, 54*(11), 6878-6887. https://doi.org/10.1021/acs.est.9b05883.

Kanellos, F. D. (2020). Optimal scheduling and real-time operation of distribution networks with high penetration of plug-in electric vehicles. *IEEE Systems Journal, 15*(3), 3938-3947. https://doi.org/10.1109/JSYST.2020.3006002.

Kostis, P., Dincer, H., & Yüksel, S. (2023). Knowledge-based energy investments of European economies and policy recommendations for sustainable development. *Journal of the Knowledge Economy, 14*(3), 2630-2662. https://doi.org/10.1007/s13132-022-00972-5.

Lee, J. O., Kim, Y. S., & Moon, S. I. (2020). Current injection power flow analysis and optimal generation dispatch for bipolar DC microgrids. *IEEE Transactions on Smart Grid, 12*(3), 1918-1928. https://doi.org/10.1109/TSG.2020.3046733.

Li, Q., Zhang, X., Guo, J., Shan, X., Wang, Z., Li, Z., & Chi, K. T. (2021). Integrating reinforcement learning and optimal power dispatch to enhance power grid resilience. *IEEE Transactions on Circuits and Systems II: Express Briefs, 69*(3), 1402-1406. https://doi.org/10.1109/TCSII.2021.3131316.

Li, X., Ma, R., Gan, W., & Yan, S. (2020). Optimal dispatch for battery energy storage station in distribution network considering voltage distribution improvement and peak load shifting. *Journal of Modern Power Systems and Clean Energy, 10*(1), 131-139. https://doi.org/10.35833/MPCE.2020.000183.

Li, Z., Wu, L., Xu, Y., Moazeni, S., & Tang, Z. (2021). Multi-stage real-time operation of a multi-energy microgrid with electrical and thermal energy storage assets: A data-driven MPC-ADP approach. IEEE *Transactions on Smart Grid, 13*(1), 213-226. https://doi.org/10.1109/TSG.2021.3119972.

Liu, H., Li, J., & Ge, S. (2020). Research on hierarchical control and optimisation learning method of multi-energy microgrid considering multi-agent game. *IET Smart Grid, 3*(4), 479-489. https://doi.org/10.1049/iet-stg.2019.0268.

Liu, J., Chen, Y., Duan, C., Lin, J., & Lyu, J. (2020). Distributionally robust optimal reactive power dispatch with Wasserstein distance in active distribution network. *Journal of Modern Power Systems and Clean Energy, 8*(3), 426-436. https://doi.org/10.35833/MPCE.2019.000057.

Liu, L. N., & Yang, G. H. (2021). Distributed optimal economic environmental dispatch for microgrids over time-varying directed communication graph. *IEEE Transactions on Network Science and Engineering, 8*(2), 1913-1924. https://doi.org/10.1109/TNSE.2021.3076526.

Liu, Z., Yi, Y., Yang, J., Tang, W., Zhang, Y., Xie, X., & Ji, T. (2020). Optimal planning and operation of dispatchable active power resources for islanded multi-microgrids under decentralised collaborative dispatch framework. *IET Generation, Transmission & Distribution, 14*(3), 408-422. https://doi.org/10.1049/iet-gtd.2019.0796.

Maka, A. O. M., & Alabid, J. M. (2022). Solar energy technology and its roles in sustainable development. *Clean Energy, 6*(3), 476-483. https://doi.org/10.1093/ce/zkac023.

Masrur, H., Shafie-Khah, M., Hossain, M. J., & Senjyu, T. (2022). Multi-energy microgrids incorporating EV integration: Optimal design and resilient operation. *IEEE Transactions on Smart Grid, 13*(5), 3508-3518. https://doi.org/10.1109/TSG.2022.3168687.

Moradzadeh, M., & Abdelaziz, M. M. A. (2020). A new MILP formulation for renewables and energy storage integration in fast charging stations. IEEE *Transactions on Transportation Electrification, 6*(1), 181-198. https://doi.org/10.1109/TTE.2020.2974179.

Nagarajan, K., Parvathy, A. K., & Rajagopalan, A. (2020). Multi-objective optimal reactive power dispatch using levy interior search algorithm. International Journal on *Electrical Engineering and Informatics, 12*(3), 547-570. https://doi.org/10.15676/ijeei.2020.12.3.8.

Naughton, J., Wang, H., Cantoni, M., & Mancarella, P. (2021). Co-optimizing virtual power plant services under uncertainty: A robust scheduling and receding horizon dispatch approach. *IEEE Transactions on Power Systems, 36*(5), 3960-3972. https://doi.org/10.1109/TPWRS.2021.3062582.

Nosratabadi, S. M., Hemmati, R., & Khajouei Gharaei, P. (2021). Optimal planning of multi-energy microgrid with different energy storages and demand responsive loads utilizing a technical-economic-environmental programming. International Journal of *Energy Research, 45*(5), 6985-7017. https://doi.org/10.1002/er.6286.

Nowak, S., Chen, Y. C., & Wang, L. (2020). Measurement-based optimal DER dispatch with a recursively estimated sensitivity model. *IEEE Transactions on Power Systems, 35*(6), 4792-4802. https://doi.org/10.1109/TPWRS.2020.2998097.

Shaheen, M. A. M., Hasanien, H. M., & Alkuhayli, A. (2021). A novel hybrid GWO-PSO optimization technique for optimal reactive power dispatch problem solution. *Ain Shams Engineering Journal, 12*(1), 621-630. https://doi.org/10.1016/j.asej.2020.07.011.

Shinde, P., Hesamzadeh, M. R., Date, P., & Bunn, D. W. (2020). Optimal dispatch in a balancing market with intermittent renewable generation. *IEEE Transactions on Power Systems, 36*(2), 865-878. https://doi.org/10.1109/TPWRS.2020.3014515.

Shirzadi, N., Nasiri, F., El-Bayeh, C., & Eicker, U. (2022). Optimal dispatching of renewable energy-based urban microgrids using a deep learning approach for electrical load and wind power forecasting. *International Journal of Energy Research, 46*(3), 3173-3188. https://doi.org/10.1002/er.7374.

Su, Y., & Teh, J. (2022). Two-stage optimal dispatching of AC/DC hybrid active distribution systems considering network flexibility. Journal of Modern *Power Systems and Clean Energy, 11*(1), 52-65. https://doi.org/10.35833/MPCE.2022.000424.

Tian, L., Cheng, L., Guo, J., & Wu, K. (2020). System modeling and optimal dispatching of multi-energy microgrid with energy storage. *Journal of Modern Power Systems and Clean Energy, 8*(5), 809-819. https://doi.org/10.35833/MPCE.2020.000118.

Vasilj, J., Jakus, D., & Sarajcev, P. (2020). Robust nonlinear economic MPC based management of a multi energy microgrid. *IEEE Transactions on Energy Conversion, 36*(2), 1528-1536. https://doi.org/10.1109/TEC.2020.3046459.

Wu, C., Gu, W., Zhou, S., & Chen, X. (2021). Coordinated optimal power flow for integrated active distribution network and virtual power plants using decentralized algorithm. *IEEE Transactions on Power Systems, 36*(4), 3541-3551. https://doi.org/10.1109/TPWRS.2021.3049418.

Xu, Y., Liu, Z., Zhang, C., Ren, J., Zhang, Y., & Shen, X. (2021). Blockchain-based trustworthy energy dispatching approach for high renewable energy penetrated power systems. *IEEE Internet of Things Journal, 9*(12), 10036-10047. https://doi.org/10.1109/JIOT.2021.3117924.

Yang, X., Xu, C., He, H., Yao, W., Wen, J., & Zhang, Y. (2020). Flexibility provisions in active distribution networks with uncertainties. *IEEE Transactions on Sustainable Energy, 12*(1), 553-567. https://doi.org/10.1109/TSTE.2020.3012416.

Yapici, H. (2021). Solution of optimal reactive power dispatch problem using pathfinder algorithm. *Engineering Optimization, 53*(11), 1946-1963. https://doi.org/10.1080/0305215X.2020.1839443.

Yodo, N., & Arfin, T. (2021). A resilience assessment of an interdependent multi-energy system with microgrids. *Sustainable and Resilient Infrastructure, 6*(2), 42-55. https://doi.org/10.1080/23789689.2019.1710074.

Zhang, Z., Wang, C., Lv, H., Liu, F., Sheng, H., & Yang, M. (2021). Day-ahead optimal dispatch for integrated energy system considering power-to-gas and dynamic pipeline networks. *IEEE Transactions on Industry Applications, 57*(4), 3317-3328. https://doi.org/10.1109/TIA.2021.3076020.

Zhao, Q., Liao, W., Wang, S., & Pillai, J. R. (2020). Robust voltage control considering uncertainties of renewable energies and loads via improved generative adversarial network. *Journal of Modern Power Systems and Clean Energy, 8*(6), 1104-1114. https://doi.org/10.35833/MPCE.2020.000210.